Bypass Transition to Sustained Thermoacoustic Oscillations in a Linearly Stable Rijke Tube

Matthew P. Juniper* and Iain C. Waugh†

Engineering Department, University of Cambridge, CB2 1PZ, United Kingdom.

In this paper we examine triggering in a simple linearly-stable thermoacoustic system using techniques from flow instability and optimal control. Firstly, for a noiseless system, we find the initial states that have highest energy growth over given times and from given energies. Secondly, by varying the initial energy, we find the lowest energy that just triggers to a stable periodic solution. We show that the corresponding initial state grows first towards an unstable periodic solution and, from there, to the stable periodic solution. This exploits linear transient growth, which arises due to nonnormality in the governing equations and is directly analogous to bypass transition to turbulence. Thirdly, we introduce noise that has similar spectral characteristics to this initial state. We show that, when triggering from low noise levels, the system grows to high amplitude self-sustained oscillations by first growing towards the unstable periodic solution of the noiseless system. This helps to explain the experimental observation that linearly-stable systems can trigger to self-sustained oscillations even with low background noise.

Nomenclature

E	acoustic energy
E_0	initial acoustic energy
F_{1G}	acoustic momentum equation
F_{2G}	acoustic energy equation
G	maximum acoustic energy growth over a given time
G_{max}	maximum acoustic energy growth over all times
j	mode number
$\mathcal{J}$	cost functional
$\mathcal{L}$	Lagrangian functional
N	total number of modes
t	time
T	optimization time
u_f	velocity at the hot wire
$\mathbf{u}$	state vector containing η_1 to η_N
$\mathbf{p}$	state vector containing η_1/π to $\eta_N/N\pi$
$\mathbf{x}$	state vector containing $(\mathbf{u};\mathbf{p})$
$\mathbf{x}_0$	initial state vector
x_f	position of the hot wire within the Rijke tube (0 to 1)
β	heat release parameter
η_j	amplitude of the j^{th} mode representing velocity
$\eta_j/j\pi$	amplitude of the j^{th} mode representing pressure
τ	time delay between a velocity fluctuation and a heat release fluctuation
ζ_j	damping of the j^{th} mode
$\|\|\cdot\|\|$	2-norm

*Senior lecturer, Engineering Department, Trumpington Street, Cambridge, CB2 1PZ, United Kingdom.
†PhD student, Engineering Department, Trumpington Street, Cambridge, CB2 1PZ, United Kingdom.

I. Introduction

In the field of flow instability there has recently been a surge of interest in bypass transition to turbulence[1,2]. In brief, this is a mechanism through which a small perturbation grows transiently and then triggers turbulence even when the corresponding laminar base flow has no unstable eigenvalues. This paper explores an analogous mechanism in thermoacoustics, through which a small perturbation triggers high amplitude self-sustained oscillations even when the unperturbed system has no unstable eigenvalues. Although flow instability differs from thermoacoustics and turbulence differs from sustained oscillations, the two situations are both nonlinear and nonnormal, which suggests that the transition process could be similar.

Triggering has been observed in solid rocket motors, liquid rocket motors and laboratory experiments[3−5]. Triggering is usually caused by large amplitude disturbances, such as a bomb placed within a combustion chamber. This is easy to explain: if a system can support large amplitude self-sustained oscillations and is given a large amplitude pulse, it can be attracted towards this oscillating state. Triggering can also arise from small amplitude disturbances, of order of the background noise level[4(Ch.1)]. This is harder to explain: how could some initial states grow to large amplitude self-sustained oscillations even though the system is linearly stable and the states' initial energy is only a small fraction of the final energy?

A clue to this may lie in hydrodynamics. In many eigenvalue-stable laminar flows, such as Poiseuille and Couette flow at moderate Reynolds number, certain initial perturbations grow transiently before they eventually decay[6]. The perturbation kinetic energy increases by a factor of around 1000 during this transient period[7]. This growth arises because the eigenfunctions of the linearized stability operator are nonorthogonal. (Non-orthogonal eigenfunctions are a feature of nonnormal operators; a matrix or operator $\mathbf{L}$ is nonnormal if it does not satisfy $\mathbf{L}^+\mathbf{L} = \mathbf{L}\mathbf{L}^+$, where $\mathbf{L}^+$ is the adjoint of $\mathbf{L}$.) This means that some initial states comprise eigenfunctions with large amplitudes that largely cancel out. If the eigenfunctions of such states decay at different rates, the states grow initially even though all the eigenfunctions eventually decay.[2] When the nonlinear development is taken into account, these can trigger turbulence in the manner described by simple models[1,8].

In flow instability, bypass transition can be divided conceptually into five stages.[9] The first stage is initiation of small perturbations to the flow. The second stage is linear amplification of these perturbations due to nonnormal growth, as described above. The third stage is nonlinear saturation into a new steady or quasi-steady periodic state. The fourth stage is growth of secondary instabilities on top of this periodic base flow. The fifth stage is breakdown to turbulence, where nonlinearities and/or symmetry-breaking instabilities excite an increasing number of scales in the flow. This idealization provides a useful framework with which to view bypass transition, even for complicated flows.

A similar framework can be used for thermoacoustics. Stage 2 will be similar because the eigenfunctions of the linearized thermoacoustic stability operator are also nonorthogonal[10] and can therefore lead to transient growth[11,12]. Thermo-acoustic systems are nonlinear so they will saturate to new steady or quasi-steady states, as in stage 3, although these states could be considerably simpler than those found in fluid mechanics. Stage 4 will be similar if the quasi-steady states found in stage 3 are unstable and subsequently lead to high amplitude self-sustained oscillations. Stage 5, breakdown to turbulence, would not be expected in thermoacoustic systems.

The aim of this paper is to study the triggering mechanism in a simple model of the horizontal Rijke tube, particularly when initiated from low initial amplitudes. The initial state that causes maximum energy growth will be calculated over a wide range of initial energies using nonlinear adjoint looping[13]. The evolution from low energy initial states will be compared with the sequence of events found during bypass transition to turbulence. Finally, the evolution will be calculated in the presence of varying degrees of background noise in order to see whether a noisy system follows the same sequence of events during triggering. This will allow a better comparison with experimental data.

II. The model of the horizontal Rijke tube

The thermoacoustic system examined in this paper is a horizontal Rijke tube[11,13]. (Further details can be found in these references.) This is a tube in which a hot wire is placed distance x_f from one end and through which a base flow is imposed. The heat release at the wire is characterized by a parameter, β, which can be thought of as a nondimensional wire temperature. Surface heat transfer, convection and diffusion between the wire and the fluid is modelled by a constant time delay, τ, between the time when the

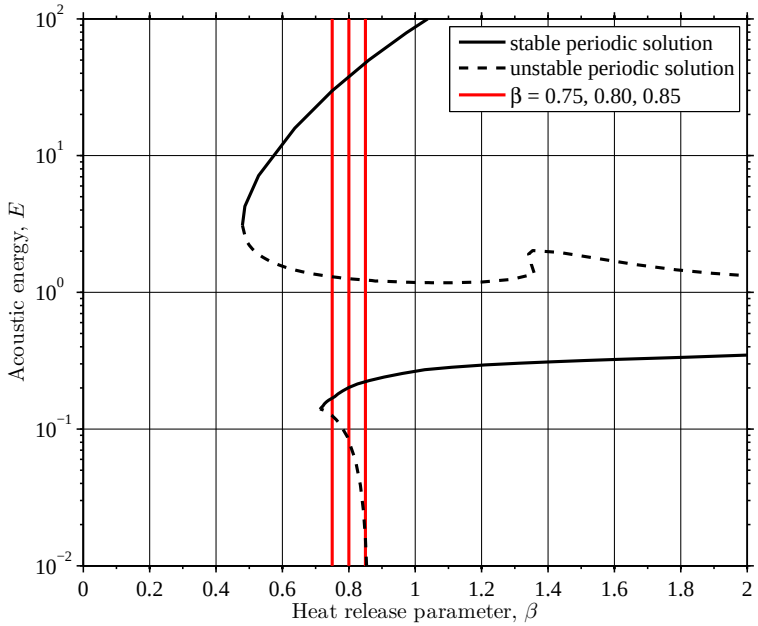

Figure 1. Bifurcation diagram for the thermoacoustic system in this paper. E is the minimum energy on the respective periodic solution and β is the heat release parameter. There are two pairs of periodic solutions: the lower, at $E < 0.5$, in which the amplitude of the perturbation velocity is less than the mean flow velocity, and the upper, at $E > 0.5$, in which the amplitude of the perturbation velocity is greater than the mean flow velocity. The red lines show the values of β examined in this paper.

velocity acts and the time when the corresponding heat release is felt by the perturbation. This system can support self-sustained thermoacoustic oscillations. The nondimensionalized governing equations, which are for evolution of the velocity and pressure perturbations, are nonlinear Delay Differential Equations (DDEs). These are discretized by projecting onto the fundamental acoustic modes of the tube. The discretized nonlinear governing equations for each mode, j are:

$$F_{1G} \equiv \frac{\mathrm{d}}{\mathrm{d}t}\eta_j - j\pi\left(\frac{\dot{\eta}_j}{j\pi}\right) = 0, \tag{1}$$

$$F_{2G} \equiv \frac{\mathrm{d}}{\mathrm{d}t}\left(\frac{\dot{\eta}_j}{j\pi}\right) + j\pi\eta_j + \zeta_j\left(\frac{\dot{\eta}_j}{j\pi}\right) + 2\beta\left(\left|\frac{1}{3} + u_f(t-\tau)\right|^{\frac{1}{2}} - \left(\frac{1}{3}\right)^{\frac{1}{2}}\right)\sin(j\pi x_f) = 0, \tag{2}$$

where

$$u_f(t-\tau) = \sum_{k=1}^{N} \eta_k(t-\tau)\cos(k\pi x_f). \tag{3}$$

The state of the system is given by the amplitudes of the Galerkin modes that represent velocity, η_j, and those that represent pressure, $\dot{\eta}_j/j\pi$. These are given the notation $\mathbf{u} \equiv (\eta_1, \ldots, \eta_N)^T$ and $\mathbf{p} \equiv (\dot{\eta}_1/\pi, \ldots, \dot{\eta}_N/N\pi)^T$. The state vector of the discretized system is the column vector $\mathbf{x} \equiv (\mathbf{u}; \mathbf{p})$. The parameters of the system are the time delay, τ, the heat release, β, the flame position, x_f and the damping coefficients, ζ_j. The values used in this paper are $\tau = 0.02$, $\beta = 0.75, 0.80, 0.85$, $x_f = 0.3$ and $\zeta_j = 0.05j^2 + 0.01j^{1/2}$ with 10 modes. These values are typical of a laboratory-scale Rijke tube[14].

Although the nonlinear DDEs (1–3) are used in this paper, it is worth mentioning that they can be linearized in two steps. The first step is to linearize the square root term, which generates a set of linear DDEs called the 'velocity-linearized' system. The second step is to linearize the time delay, which generates a set of linear Ordinary Differential Equations ODEs called the 'fully-linearized' system. The fully-linearized governing equations are nonself-adjoint, which means that their corresponding eigenfunctions are nonorthogonal and can therefore cause nonnormal transient growth even when the system is linearly stable.[11]

In this paper, the magnitude of the acoustic oscillations is quantified by the acoustic energy per unit

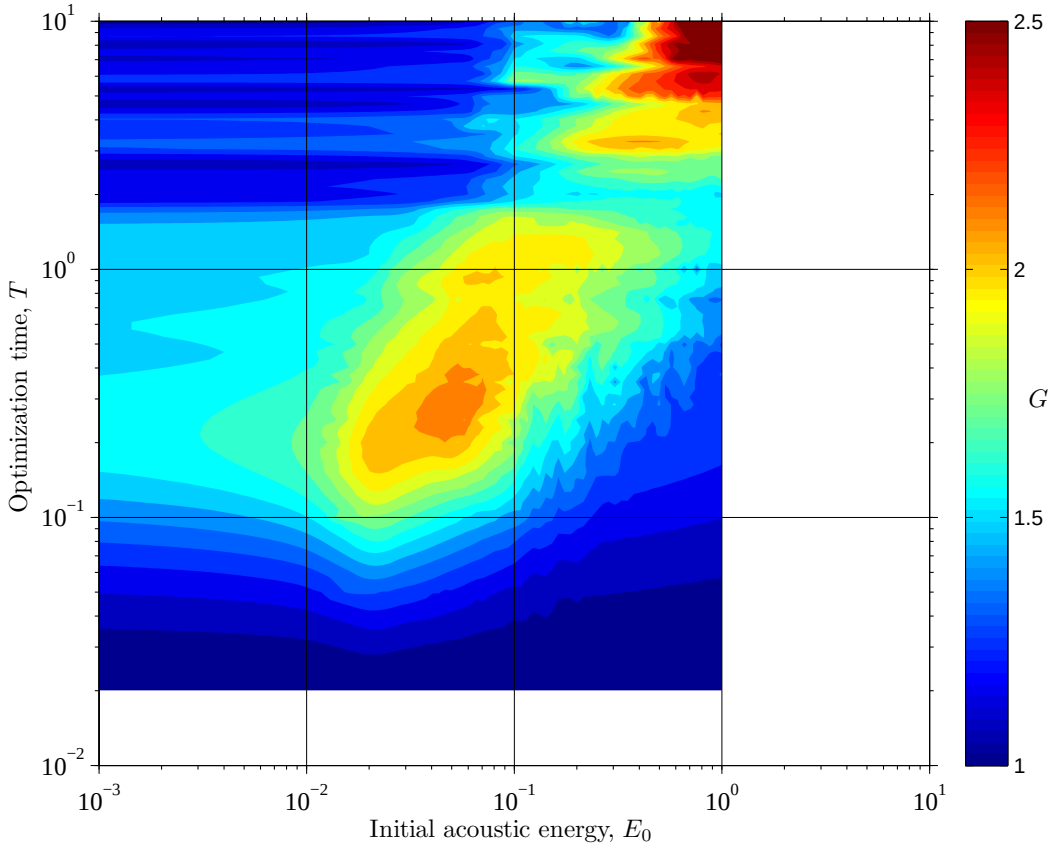

Figure 2. Contours of G in the (T, E_0)-plane for the system with $\beta = 0.75$, found with nonlinear adjoint looping[18]. There are several local maxima. One maximum, which occurs at moderate T and moderate E_0, corresponds to initial states that are similar to the linear optimal. Other maxima, which occur at large T and large E_0, correspond to initial states that grow to self-sustained oscillations.

volume, where $||\cdot||$ denotes the 2-norm:

$$E = \frac{1}{2}u^2 + \frac{1}{2}p^2 = \frac{1}{2}\sum_{j=1}^{N}\eta_j^2 + \frac{1}{2}\sum_{j=1}^{N}\left(\frac{\dot{\eta}_j}{j\pi}\right)^2 = \frac{1}{2}\mathbf{x}^H\mathbf{x} = \frac{1}{2}||\mathbf{x}||^2. \tag{4}$$

III. The Bifurcation diagram

The bifurcation diagram for this system, calculated with a continuation method[13,15,16], is shown in Fig. 1. Each point on each line corresponds to a periodic solution, the minimum energy of which is plotted. There are two pairs of solutions: the lower, at $E < 0.5$, in which the amplitude of the perturbation velocity is less than the mean flow velocity, and the upper, at $E > 0.5$, in which the amplitude of the perturbation velocity is greater than the mean flow velocity. For $\beta < 0.859$, there is a stable fixed point at zero amplitude. At the linear stability threshold, $\beta = 0.859$, there is a subcritical Hopf bifurcation to the lower unstable periodic solution. This unstable periodic solution becomes the lower stable periodic solution at the lower saddle node bifurcation at $\beta = 0.714$. Similarly, the upper unstable periodic solution becomes the upper stable periodic solution at the upper saddle node bifurcation at $\beta = 0.485$. For β between the saddle node bifurcations and the Hopf bifurcation, the system is susceptible to triggering. This range of β is also known as 'linearly stable but nonlinearly unstable'.

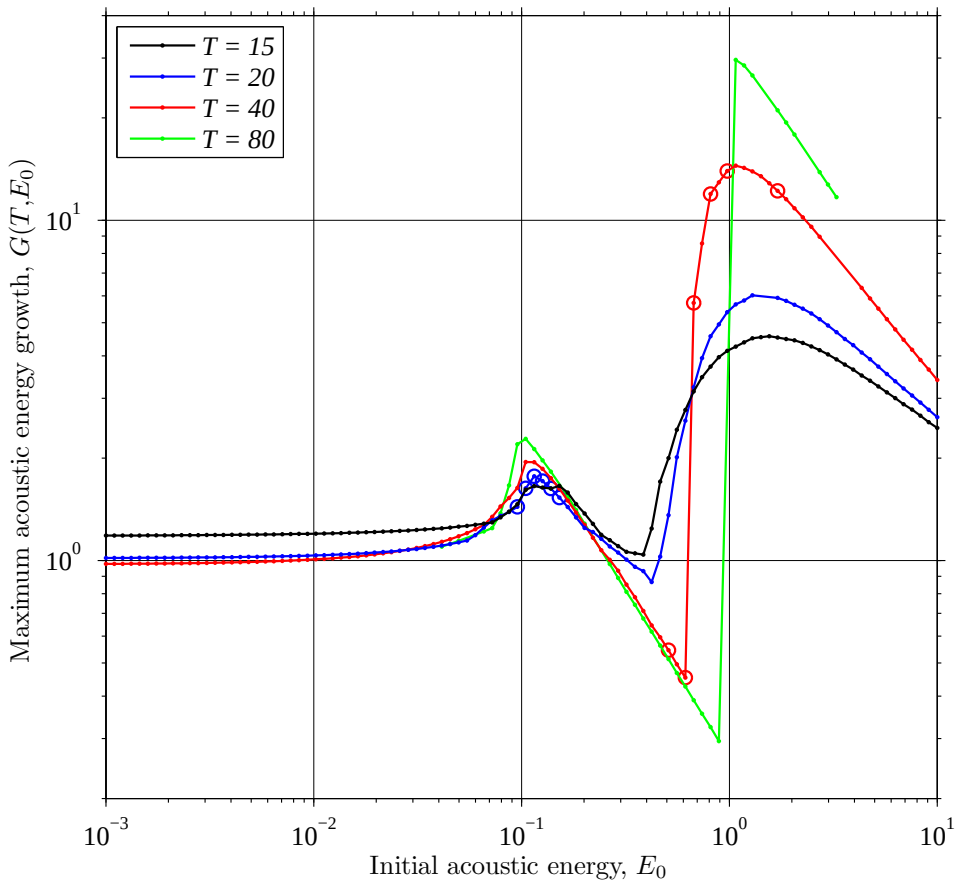

Figure 3. Maximum growth rate, $G(T, E_0)$, over a wide range of initial energies, E_0, at times $T = 15, 20, 40, 80$ for the system with $\beta = 0.75$. There are two maxima. One occurs at $E_0 \sim 0.1$ and has small G_{max}. The other occurs at $E_0 \sim 1$ and has large G_{max}. As the optimization time increases, the two maxima become sharper and more distinct. The blue and red circles show the initial states whose evolution is shown in Figs. 4 and 5.

IV. Finding linear and nonlinear optimal initial states

The optimal initial state is defined as the initial state that has the maximum acoustic energy growth over a given time, T. This growth is given the symbol G:

$$G(T) = \max_{\mathbf{x}_0} \frac{||\mathbf{x}(T)||^2}{||\mathbf{x}_0||^2}. \tag{5}$$

In the linear system, G is a function only of T. For this system, the maximum possible value of G can be found by performing a second optimization in T. This optimum is given the symbol G_{max} and the time at which it occurs is given the symbol T_{max}. The optimal initial state of the linearized system, which gives rise to $G(T)$, can be found easily from the Singular Value Decomposition (SVD) of the linearized governing equations expressed in matrix form[2,11]. This is not the same, however, as the optimal initial state of the nonlinear system, which cannot be found from the SVD.

The technique used in this paper to find the optimal initial state of the nonlinear governing equations is adapted from optimal control[13,17]. In brief, a cost functional, $\mathcal{J}$, is defined. It is convenient if this is the acoustic energy at time T divided by the initial acoustic energy, in which case the optimal value of $\mathcal{J}$ is simply equal to G. A Lagrangian functional, $\mathcal{L}$, is then defined as the cost functional, $\mathcal{J}$, minus a set of inner products. These inner products multiply the governing equations by one set of Lagrange multipliers and the initial state by another set of Lagrange multipliers. When all variations of $\mathcal{L}$ with respect to the Lagrange multipliers, state variables, $\mathbf{x}$, and initial state, $\mathbf{x}_0$, are zero then an initial state has been found that optimizes $\mathcal{J}$ and satisfies the governing equations. This process finds local optima. Another optimization routine is required to find the global optimum. In this paper, local optima are found from 100 randomly-chosen initial

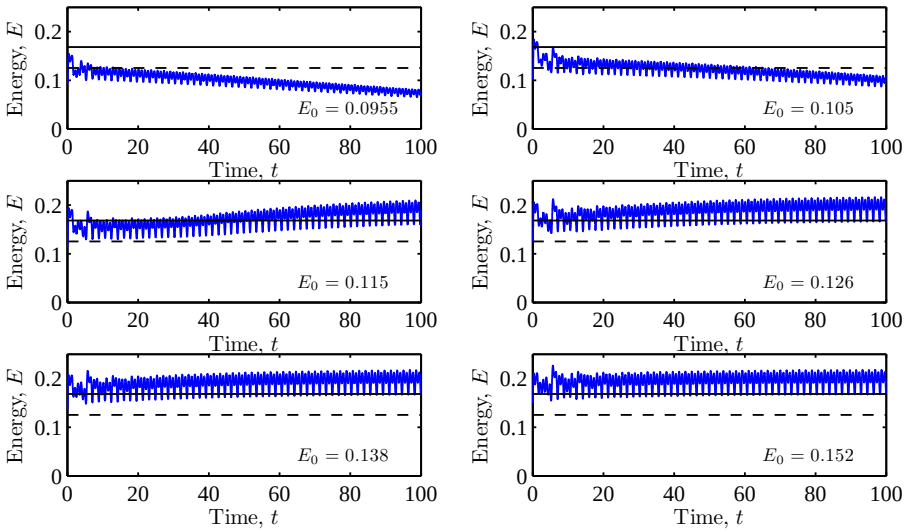

Figure 4. Evolution of the acoustic energy, $E(t)$, from the optimal initial states at $E_0 \sim 0.1$ and $T = 20$, circled blue in Fig. 3. The solid black line shows the minimum energy on the lower stable periodic solution. The dashed black line shows the minimum energy on the lower unstable periodic solution. The top two frames show initial states that evolve directly towards the stable fixed point at zero. The bottom two frames show initial states that evolve directly towards the stable periodic solution. The third frame (middle left) shows an initial state that initially evolves towards the lower unstable periodic solution and then grows towards the lower stable periodic solution.

states. This is robust but is not computationally efficient. It is highly likely that a better procedure could be found.

V. Non-linear optimal initial states

In the linearized systems, G is a function only of T. In the nonlinear system, G is also a function of the initial state's amplitude, which in this paper is quantified by the initial acoustic energy, E_0. Figure 2 shows a map of $G(T, E_0)$ for the case with $\beta = 0.75$, taken from Ref. 18. This reveals that G has several local maxima. One maximum, which occurs at moderate T and moderate E_0, corresponds to initial states that are similar to the linear optimal. Other maxima, which occur at large T and large E_0, correspond to initial states that grow to self-sustained oscillations[18]. The aim of this paper is to explore the maxima at large T and large E_0.

The maximum growth, $G(T, E_0)$, for long optimization times ($T = 15, 20, 40, 80$) and high initial energies is shown in Fig. 3. This extends beyond the top right corner of Fig. 2. There are two maxima. One occurs at $E_0 \sim 0.1$ and has small G_{max}. The other occurs at $E_0 \sim 1$ and has large G_{max}. As the optimization time increases, the two maxima become sharper and more distinct.

Figure 4 shows the evolution of the acoustic energy from some optimal initial states near the first maximum on Fig. 3. In all cases, there is strong transient growth in the first cycle, which can be seen at the far left of each frame. In the top two frames, the energy subsequently decays to the zero fixed point. In the bottom four frames, the energy subsequently grows to the stable periodic solution. From this figure, it can be seen that the triggering threshold lies between $E_0 = 0.105$ and $E_0 = 0.115$.

In the third frame of Fig. 4, for which $E_0 = 0.115$, the system is initially attracted towards the unstable periodic solution before growing to the stable periodic solution. This reveals the significance of the unstable periodic solution to triggering from low initial energies[13,18]. The unstable periodic solution is a loop that sits on the boundary between the basins of attraction of the stable periodic solution and the stable fixed point. All but one of its Floquet multipliers are stable, which means that it attracts locally in every direction but one. No other periodic solutions or fixed points exist on the basin boundary, which means that all states exactly on the basin boundary must be attracted towards the unstable periodic solution. All states very slightly off the basin boundary follow neighbouring trajectories towards the unstable periodic solution but are then repelled either to the stable fixed point or to the stable periodic solution. In other words, all low energy triggering events must pass very close to the unstable periodic solution. The third frame of Fig. 4

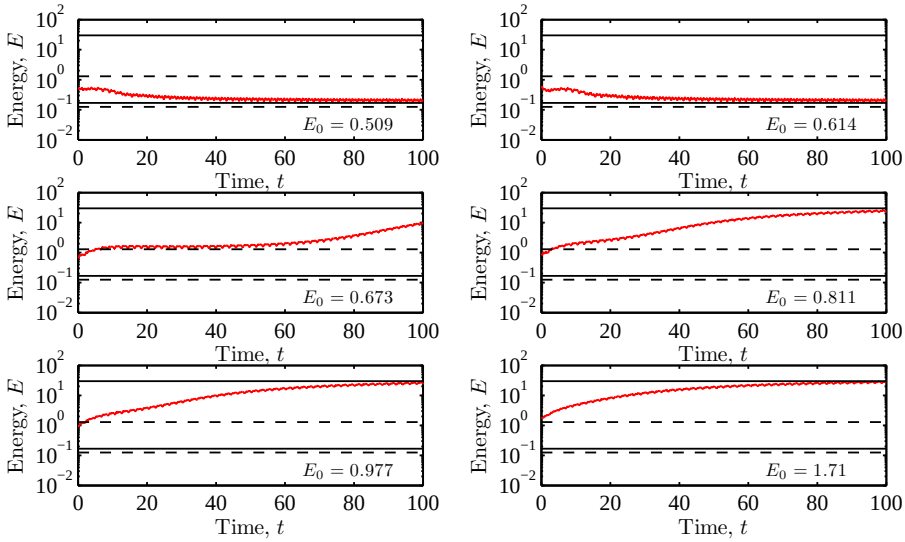

Figure 5. Evolution of the acoustic energy, $E(t)$, from the optimal initial states at $E_0 \sim 1$ and $T = 40$, circled red in Fig. 3. The solid black lines show the minimum energy on the lower and upper stable periodic solutions. The dashed black lines show the minimum energy on the lower and upper unstable periodic solutions. The top two frames show initial states that evolve directly towards the lower stable periodic solution. The bottom two frames show initial states that evolve directly towards the upper stable periodic solution. The third frame (middle left) shows an initial state that initially evolves towards the upper unstable periodic solution and then grows towards the upper stable periodic solution.

shows an example of such a trajectory.

Figure 5 shows the evolution of the acoustic energy from some optimal initial states near the second maximum on Fig. 3. In the top two frames, the energy decays to the lower stable periodic solution. In the bottom four frames, the energy grows to the upper stable periodic solution. It can be seen that the threshold for triggering to the upper stable periodic solution lies between $E_0 = 0.614$ and $E_0 = 0.673$. For the same reasons as before, all low energy triggering events to the upper stable periodic solution must pass very close to the upper unstable periodic solution. The third frame of Fig. 5 shows an example of such a trajectory. The same qualitative behaviour is found for the case with $\beta = 0.80$, which is shown in Fig. 6.

The shape of $G(T, E_0)$ in Fig. 3 can now be explained. The first maximum, at $E_0 \sim 0.1$, corresponds to initial states that are close to the basin boundary between the stable fixed point and the lower stable periodic solution. Around the triggering threshold, these states are attracted first towards the lower unstable periodic solution, which lies on this basin boundary, before subsequently being attracted to one of the stable solutions. The energy on the unstable periodic solution oscillates from $E = 0.125$ (Fig. 1) to $E = 0.163$ so this attraction involves either transient energy growth, which accounts for the peak at $E_0 \sim 0.11$, or transient energy decay, which accounts for the trough at slightly higher E_0. The transient energy growth towards this unstable periodic solution arises from nonnormality in the linearized governing equations[13]. The second maximum, at $E_0 \sim 1$, corresponds to the same behaviour around the upper unstable periodic solution. As the optimization time increases, the trajectory becomes closer to its final destination, which means that the peaks and troughs become sharper. For very long optimization times, at which the final energy must take one of three values, $G(T, E_0)$ will have a saw-tooth profile with a vertical ramp at both triggering thresholds, as is beginning to be seen in the line for $T = 80$.

In summary, for values of β between the saddle node bifurcations and the Hopf bifurcation, any initial state must sit within the basin of attraction of either the stable fixed point or a stable periodic solution (except for states exactly on the basin boundary). If the initial state is far from the basin boundary, as is usually the case, its evolution towards a stable solution is straightforward. This corresponds to the triggering from high amplitudes that is readily seen experimentally. If the initial state is close to the basin boundary, however, it evolves to its final state by firstly passing close to the unstable periodic solution, which sits on the basin boundary. Crucially, some states grow transiently towards the unstable periodic solution and then to the stable periodic solution even when they have quite low initial energies. The stages of this evolution corresponds closely to stages 2, 3 and 4 seen in bypass transition to turbulence[9]. The corresponding initial

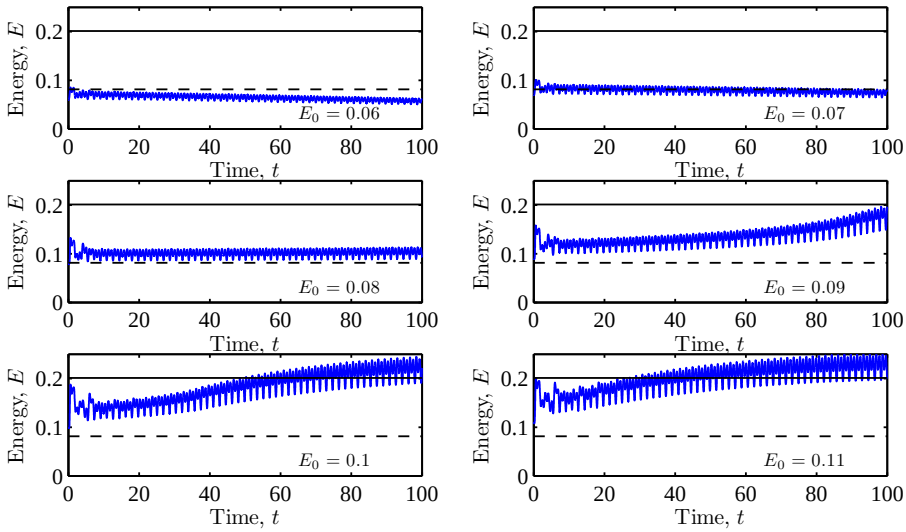

Figure 6. As for Fig. 4 but for the system with $\beta = 0.80$. This has the same qualitative behaviour as the system with $\beta = 0.75$ but the stable and unstable periodic solutions are further apart.

states, which are called the 'most dangerous' initial states, are found with the nonlinear adjoint looping algorithm outlined here with a long optimization time. This gives the same result as that found by working backwards from the unstable periodic solution[13,18].

VI. Triggering by background noise

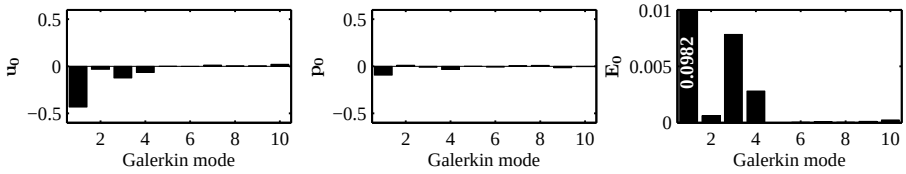

Figure 7. The most dangerous initial state for the system with $\beta = 0.75$. Of all the states that can reach the stable lower periodic solution, this is the one with the lowest energy. Most of its energy is in the first mode, but a significant amount is in modes 2 3 and 4.

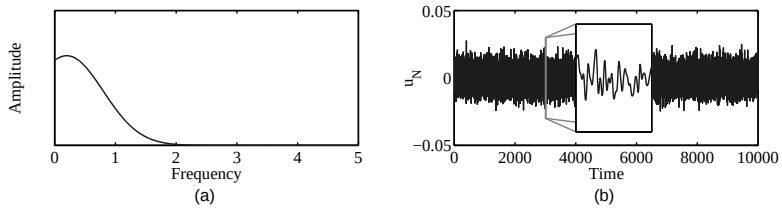

Figure 8. The noise profile imposed on the Rijke tube in (a) the frequency domain and (b) the time domain, with a strength of 0.5%. The inset in (b) is 20 time units long. This noise profile has been chosen because it has similar spectral characteristics to the most dangerous initial state in Fig. 7. The first mode in Fig. 7 has frequency 0.5.

It is unrealistic to assume that a perfectly known initial state could be imposed on a perfectly quiet Rijke tube, as is modelled in section V to reveal the triggering mechanism. It is more realistic to include background noise, whose amplitude and spectral characteristics can be well-defined, and to examine how this noise causes triggering. This paper considers additive noise, where a small stochastic perturbation is added continually to the system, in this case to the velocity at the flame. Other types of noise are parametric

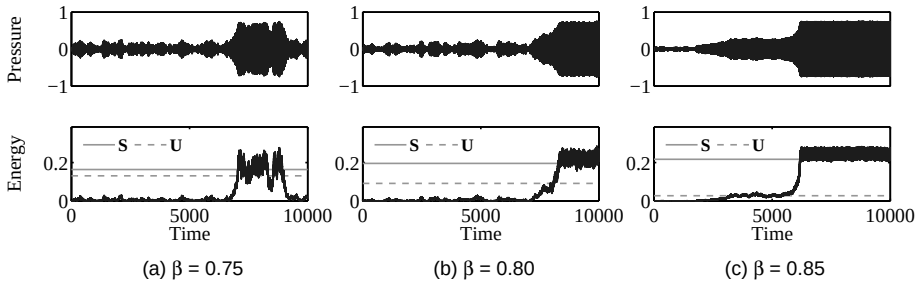

Figure 9. The evolution of pressure and energy for the system at three different noise amplitudes and β values: (a) 1.2% noise with $\beta = 0.75$, (b) 0.73% noise with $\beta = 0.80$ and (c) 0.25% noise with $\beta = 0.85$. The solid straight line shows the minimum energy of the lower stable periodic solution. The dashed straight line shows the minimum energy of the lower unstable periodic solution. Frame (a) shows direct triggering to the stable periodic solution. Frames (b) and (c) show triggering via the unstable periodic solution.

noise, where coefficients in the governing equations vary, and multiplicative noise, where noise amplitude is proportional to the current state of the system.

Figure 7 shows the most dangerous initial state for triggering to the lower stable periodic solution for $\beta = 0.75$. This has highest energy in the first mode, with a small but significant amount in the third and fourth modes. The noise profile that will project most successfully onto this state has high amplitudes at lower frequencies, which is labelled pink noise. In numerical simulations[19], this type of noise profile has been found to cause triggering at lower amplitudes than noise whose frequency spectrum is flat (white noise) or one that has high amplitudes at high frequencies (blue noise). In this paper the pink noise profile shown in Fig. 8 will be imposed on the system at a variety of amplitudes and only the behaviour around the lower periodic solution will be considered. These results are reported fully in Ref. 20.

Figure 9 shows pressure and energy as a function of time for the Rijke tube model at three values of β in the range that is susceptible to triggering (i.e. that is linearly stable but nonlinearly unstable). The noise is quantified by the amplitude of the velocity fluctuations divided by the velocity of the mean flow. Figure 9(a) shows the case with $\beta = 0.75$ and noise of 1.2%. For 7000 time units, the state hovers around the stable fixed point. Then the energy suddenly increases to that of the stable periodic solution for 2000 time units and then returns to zero. This can be interpreted as the noise having caused the state to move from the basin of attraction of the stable fixed point to that of the stable periodic solution and back again. If the noise is switched off at any point, the system will relax to the stable solution in whose basin it currently sits.

Figure 9(b) shows the case with $\beta = 0.80$ and noise of 0.73%. For 8000 time units, the state hovers around the stable fixed point. Then the energy increases towards a plateau around the unstable periodic solution and, from there, grows to the stable periodic solution. Figure 9(c) shows the case with $\beta = 0.85$ and noise of 0.25%. It has the same qualitative behaviour as that in Fig. 9(b) but is less obscured by noise. This behaviour can be interpreted in the same way as before but this time the role of the unstable periodic solution can be seen. At low noise levels, the unstable periodic solution acts as a gateway between the basins of attraction of the stable fixed point and the stable periodic solution, as was seen in the noiseless case in section V. This interpretation of Figs. (b) and (c) is consistent with the experimental results in Fig. 15b of Ref. 21, in which triggering that has been induced by background or combustion noise is seen to occur in two steps: a jump to an intermediate state followed by growth to a quasi periodic solution.

VII. Conclusions

Perturbations in a thermoacoustic system can grow transiently and trigger self-sustained oscillations even when the system is linearly stable. The simple model in this paper highlights some important features of this process. For large amplitude perturbations or noise, triggering occurs when the system is knocked into a state well within the basin of attraction of the stable periodic solution (bottom frames of Figs. 4, 5 & 6 and Fig. 9a). For small amplitude perturbations or noise, triggering occurs via transient growth to an intermediate unstable periodic solution, from which the system then grows to a stable periodic state (middle frames of Figs. 4, 5 & 6 and Fig. 9b-c). This is analogous to the sequence of events observed in bypass transition to turbulence in fluid mechanical systems and has the same underlying cause.

The initial states that cause maximum growth, G, after long times, T, have been calculated with nonlinear

adjoint looping[13]. As T increases, the triggering threshold can be identified increasingly accurately: it lies at the vertical jump in the saw-tooth profile of $G(E_0)$ (Fig. 3). For this system, there are two jumps. One corresponds to the triggering threshold for the lower stable periodic solution. The other corresponds to the triggering threshold for the upper stable periodic solution.

Transient growth in real thermoacoustic systems is 10^5 to 10^6 times greater than that in the Rijke tube[12]. One practical conclusion of this paper is that, even in the linearly stable regime, it may take very little noise for a real thermoacoustic system to reach high amplitude self-sustained oscillations.

Acknowledgments

We would like to thank Peter Schmid, R. I. Sujith, Satheesh Mariappan and Priya Subramanian for fruitful discussions during this project. This work was supported by the U.K. Engineering Physical and Sciences Research Council (EPSRC) and the AIM Network* through grants EP/G033803/1 and EP/GO37779/1.

References

[1]Trefethen, L.N., Trefethen, A.E., Reddy, S.C. and Driscoll, T.A. "Hydrodynamic stability without eigenvalues," *Science*, Vol. 261, 1993, pp. 578–584.

[2]Schmid, P.J. "Nonmodal Stability Theory," *Annu. Rev. Fluid Mech.*, Vol. 39, 2007, pp. 129–162.

[3]Ananthkrishnan, N., Deo, S., and Culick, F. "Reduced-order modeling and dynamics of nonlinear acoustic waves in a combustion chamber," *Combust. Sci. Tech.,* Vol. 177, 2005, pp. 221–247.

[4]Lieuwen, T. C. and Yang, V. *Combustion instabilities in gas turbine engines*, AIAA, 2005.

[5]Noiray, N., Durox, D., Schuller, T. and Candel, S. M. "A unified framework for nonlinear combustion instability analysis based on the flame describing function," *J. Fluid Mech.,* Vol. 615, 2008, pp. 139 - 167.

[6]Reddy, S. C. and Henningson, D. S. "Energy growth in viscous channel flows," *J. Fluid Mech.,* Vol. 252, 1993, pp. 209–238.

[7]Butler, K. M. and Farrell, B. F. "Three-dimensional optimal perturbations in viscous shear flow," *Phys. Fluids A,* Vol. 4, No. 8, 1992, pp. 1637–1650.

[8]Waleffe, F. "Transition in shear flows. Nonlinear normality verses nonnormal linearity," *Phys. Fluids,* Vol. 7, No. 12, 1995, pp. 3060–3066.

[9]Schmid, P.J. and Henningson, D.S. *Stability and transition in shear flows*, Springer, 2001.

[10]Nicoud, F., Benoit, L., Sensiau, C. and Poinsot, T. "Acoustic Modes in Combustors with Complex Impedances and Multidimensional Active Flames," *AIAA J.,* Vol. 45, No. 2, 2007, pp. 426–441.

[11]Balasubramanian, K. and Sujith, R.I. "Thermoacoustic instability in a Rijke tube: nonnormality and nonlinearity" *Phys. Fluids* Vol. 20, 2008, 044103.

[12]Balasubramanian, K. and Sujith, R.I. "Non-normality and nonlinearity in combustion-acoustic interaction in diffusion flames," *J. Fluid Mech.,* Vol 594, 2008, pp. 29–57.

[13]Juniper, M. P. "Triggering in the horizontal Rijke tube: nonnormality, transient growth and bypass transition," *J. Fluid Mech.,* 2010, submitted for publication.

[14]Heckl, M. "Nonlinear acoustic effects in the Rijke tube," *Acustica,* Vol. 72, 1990, p. 63.

[15]Engelborghs, K., Luzyanina, T. & Roose, D. "Numerical bifurcation analysis of delay differential equations using DDE-BIFTOOL," *ACM Trans. Math. Softw.,* Vol. 28, No.1, 2002, pp. 1 – 21.

[16]Subramanian, P., Mariappan, S., Sujith, R. I. and Wahi, P. "Application of numerical continuation to bifurcation analysis of Rijke tube," *N3L Int. Workshop on nonnormal and nonlinear effects in aero- and thermo-acoustics,* TU Munich, 2010.

[17]Bewley, T. "Flow control: new challenges for a new Renaissance," *Prog. Aerospace. Sci.,* Vol. 37, 2001, pp. 21–58.

[18]Juniper, M. P. "Transient growth in the horizontal Rijke tube: nonlinear optimal initial states," *N3L Int. Workshop on nonnormal and nonlinear effects in aero- and thermo-acoustics,* TU Munich, 2010.

[19]Waugh, I. C., Geuss, M. and Juniper, M. P. "Triggering, bypass transition and the effect of noise on a linearly stable thermoacoustic system," *Proc. Combust. Symp.,* 2010, submitted for publication.

[20]Waugh, I. C., Geuss, M. and Juniper, M. P. "Triggering in a thermoacoustic system with stochastic noise," *N3L Int. Workshop on nonnormal and nonlinear effects in aero- and thermo-acoustics,* TU Munich, 2010.

[21]Lieuwen, T. "Experimental investigation of limit-cycle oscillations in an unstable gas turbine combustor," *J. Prop. Power,* Vol. 18, No. 1, 2002, pp. 61–67.

*http://www-diva.eng.cam.ac.uk/AIM_Network/AIM_home.html